Preliminary Results of a Heat Flow Study of the Williston Basin Using Temporarily Abandoned Oil Wells, Western North Dakota

Mark R. McDonald[1], William D. Gosnold[2], and Stephan H. Nordeng[2]

[1]North Dakota Geological Survey, Bismarck ND
[2]Department of Geology and Geological Engineering, University of North Dakota, Grand Forks ND

Keywords
Heat flow, Williston Basin, temperature logging, temporarily abandoned wells, North Dakota, memory tool

ABSTRACT

The North Dakota Geological Survey (NDGS) has embarked on a temperature survey of the Williston Basin, North Dakota. To date, eleven temporarily abandoned oil and gas wells have been logged using a memory tool equipped with a temperature, gamma-ray, and casing collar locator probe lowered by a slickline. Several methods were used to estimate heat flow at the various locations including calculations based on average laboratory values of thermal conductivity, existing heat flow maps, the Bullard Method, and finding the harmonic mean of thermal conductivity. Although there is general agreement in calculated heat flow values between the various methods listed above, the results are largely predicated upon initial assumptions of either heat flow, thermal conductivity, or both.

While we are confident in the measurements obtained during this study with respect to thermal gradient, additional information on the thermal conductivity of the geologic formations will be required to estimate heat flow within the Williston Basin with better accuracy. Geologic formations can often be differentiated on the basis of "marker" beds, but there can be wide variations in mineralogy, lithology, porosity, permeability, density, etc., depending upon depositional environment, depth of burial and secondary processes from one location to another which can profoundly influence thermal conductivity and therefore greatly affect the calculated heat flow.

Introduction

In 2014, the North Dakota Geological Survey (NDGS) initiated a temperature logging program in the Williston Basin. The primary goal of the program is to gain further insight into the thermal history of the basin that may result in the development of improved models for use in exploration for oil and natural gas (Prensky, 1992). The program has also been designed to gather data useful in the evaluation of the geothermal potential of the Williston Basin. Insight into the timing of petroleum generation, migration, accumulation and preservation can be gained by determining the thermal maturity of hydrocarbons and/or by using the paleoheat flux of a sedimentary basin (Nuccio and Barker, 1990). Subsurface temperature is important to understanding the origin and evolution of sedimentary basins and can also be used in the determination of important kinetic factors as described by Nordeng and Nesheim (2011) and Nordeng (2012, 2013, 2014) that can ultimately be used to predict the oil generation potential of various geologic formations within the Williston Basin. These heat flow values represent critical data that are needed to validate and, where needed, update current heat flow maps (Blackwell and Richards, 2004). Heat flow, together with thermal conductivity values of subsurface rocks, can be used to estimate subsurface temperatures at other locations and depths. This information can also be used in the evaluation, assessment and possible exploration and development of geothermal energy in the Williston Basin.

Methodology

While subsurface temperatures are routinely collected during logging and drill stem tests, true formation temperatures are rarely recorded because drilling, well completion and production operations can cause significant variations in the wellbore temperature from the actual temperature of the neighboring strata. These temperature differences can persist for days or weeks after drilling or production has ceased. For example, during drilling, the circulation of drilling mud can cool the rock, during completion operations curing of cement and acidizing are exothermic reactions that can heat the rock, and gas entering the wellbore during production cools by expansion. In order to confidently obtain accurate subsurface temperatures, care must be taken to assure that the well bore and formation temperatures are the same, i.e. that the temperatures have equilibrated. A number of correction schemes have been derived to account for variations between actual formation temperatures and the measured wellbore temperatures obtained during drilling or while the well is producing such as that developed by Cooper and Jones (1959) or the Horner Method (Lachenbruch and Brewer, 1959). However, the best alternative is to make use of well bores that have been idle for months or, if possible, years so that equilibrated temperatures have been reached. Given these constraints and a review of the pertinent literature, the NDGS concluded that wells that have been temporarily abandoned and undisturbed for at least three months would meet the requirements of this study.

The project consisted of lowering a GOWell Model GTC43C Pegasus® temperature probe with an accuracy of 0.5ºC into eleven temporarily abandoned oil and gas wells to the bottom of the well (depth of the plug). The tool included a memory controller sub and was lowered by means of a 0.092 inch "slickline" (nonconductive cable) operated by Gibson Energy Inc. (WISCO division). The depth of the logging runs ranged between approximately 3960 m (13,000 ft) and 915 m (3,000 ft). The wells were selected based on location, depth, length of time of being undisturbed, and the ability to obtain permission from the current well operators to perform the logging. Locations of the wells are shown in Figure 1.

After setting the equipment up over a well (Figures 2 and 3), a gauge ring (dummy or slug) was lowered down to verify that there were no obstructions and to determine the maximum depth that could be logged for wells that still contained production tubing or where other potential obstructions might exist within the wellbore. After removal of the gauge ring, a period of time (generally on the order of an hour or more) was

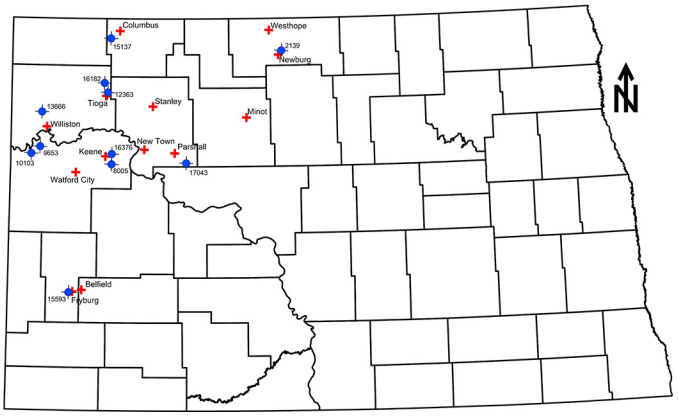

Figure 1. Location of Phase I Temporarily Abandoned Wells that were logged (blue) and nearby cities (red) in North Dakota. Numbered labels indicate the North Dakota Industrial Commission (NDIC) well number.

Figure 2. Connecting the tool to the slickline. From left to right: Mike Harden, WISCO, David Smith, WISCO, Jay Jamali, GOWell, and Kevin Hammer, WISCO.

Figure 3. Slickline unit set up over NDIC Well # 12363, Astrid Ongstad 14-22 north of Tioga, ND.

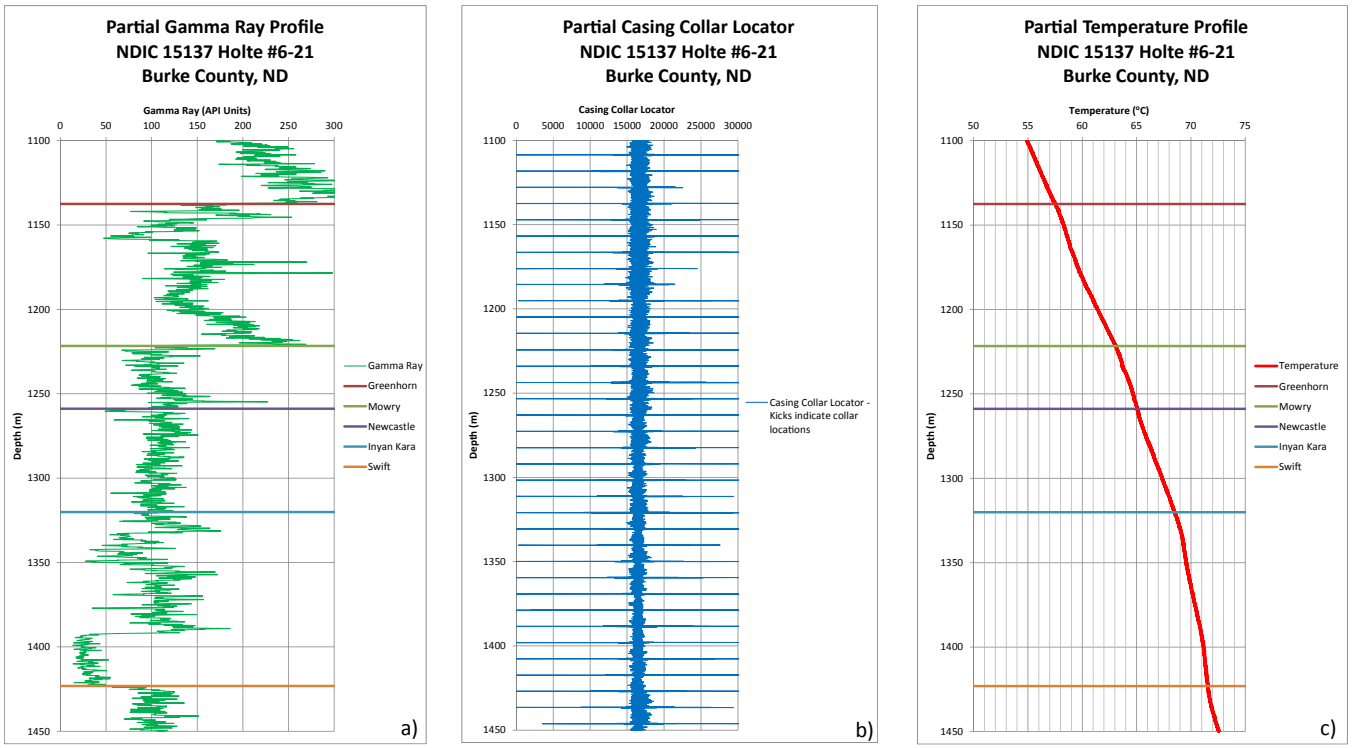

Figure 4. Partial profiles of the Holte #6-21 well: a) partial gamma ray profile illustrating formation top picks; b) partial casing collar locator profile; c) partial temperature gradient profile with formation top picks.

allowed to elapse in order for the well fluid temperatures to re-equilibrate before lowering the logging tools. For wells that were known not to contain production tubing, the gauge ring was not deployed. The wells were then logged as the tool was lowered into the well to minimize temperature disturbance or mixing of the fluids arising from the displacement of fluids by the volume of the tool. In addition to temperature, the tool was also equipped with a Casing Collar Locator (CCL) and a Gamma Ray probe to aid in correlation of the temperature probe with depth and with the geologic formations (Figure 4). As noted above, a memory controller sub was used which recorded the probe readings at a rate of one reading every 40 milliseconds (ms). The readings were downloaded to a computer after the tool was brought back to the surface. For comparison purposes, the wells were also logged on the way out of the wellbore.

Gradient or station stops were also made as the tool was lowered into the wells. In the first few wells, these stops were made more frequently (every 500 to 1000 m) to ascertain the response time of the tool in an effort to optimize the logging speed and to obtain an indication of the tool precision. An example of one of the gradient stops is presented as Figure 5. Once a reasonable logging speed was determined (20 m/min provided good results), a ten minute gradient stop was typically made at the approximate midpoint of the well and at the bottom of the logging interval for the remaining wells. The relationship between heat flow, thermal conductivity, and temperature gradient can be expressed by Fourier's Law:

$$Q = \lambda\, \Delta T/\Delta Z, \tag{1}$$

where: Q = conductive heat flow;

λ = thermal conductivity; and

$\Delta T/\Delta Z$ = temperature gradient (change of temperature over change in depth).

As presented by Nordeng (2014), this equation can be re-arranged as:

$$\Delta T = Q\, \Delta Z/\lambda. \tag{2}$$

Estimates of the temperature at depth (T_n) are found by adding the temperature changes ($\Delta T_i = QZ_i/\lambda_i$) associated with each deeper stratigraphic unit (i=1…n) to the "average" surface temperature (T_o) as follows:

$$T_n = T_o + Q\,(Z_1/\lambda_1 + Z_2/\lambda_2 + \ldots + Z_n/\lambda_n), \tag{3}$$

where:

n = number of overlying stratigraphic units in the section, where i = 1…n (the deepest layer);

T_n = temperature at the base of the n^{th} unit;

T_o = average surface temperature;
Z_n = thickness of the n^{th} unit;
l_n = thermal conductivity of the n^{th} layer.

Thus, to calculate the temperature at any point, it is necessary to know the average surface temperature, the thickness of the units (obtained from well logs), the thermal conductivities of the formations (obtained from the literature or direct measurements, e.g. Gosnold et al., 2012), and the conductive heat flow for the area (obtained from current heat flow maps, such as Blackwell and Richards, 2004). Although reasonable estimates of the average surface temperature and approximate thicknesses of the formations across the basin can be made, the biggest sources of error are caused by using inaccurate thermal conductivities or by assuming incorrect values of heat flow as current maps are based on a relatively limited dataset. Therefore, several methods were employed to calculate the heat flow using variations of equation 1, such that improved estimates of T_n can be made across the Williston Basin from equation (3). Initially, the temperature gradients measured in the wells that were logged and previously published values of thermal conductivity laboratory measurements, other literature values, and/or empirical estimates (Gosnold et al., 2012) were utilized to calculate the heat flow. The first method used was to match the graphical temperature gradient with assumed thermal conductivity and heat flow values using equation (3) above. Initially, heat flow was adjusted using the thermal conductivity values from the closest well as presented by Gosnold et al. (2012), and temperature at depth was modeled. Heat flow values were adjusted using a number of trials until the modeled temperatures were reasonably close to the measured values, as illustrated in Figure 6.

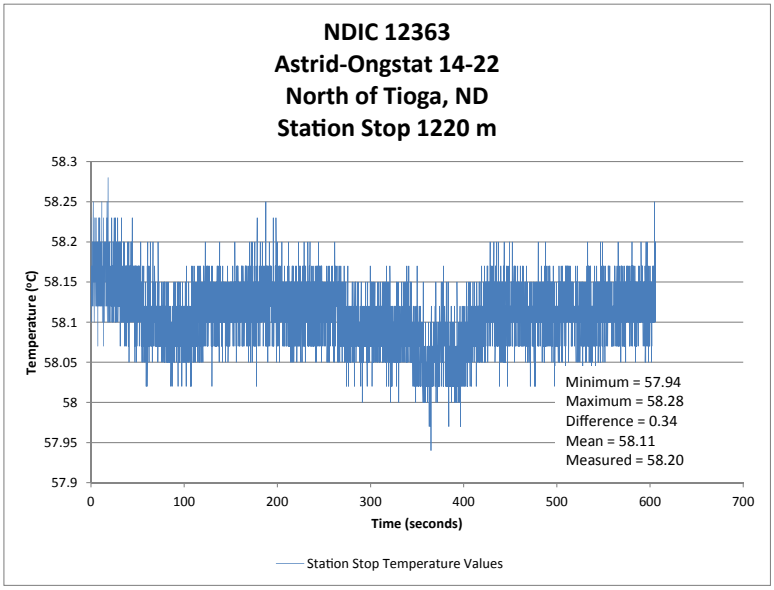

Figure 5. Variation of temperature vs. time at station stop at 1220 m (4000 ft) for NDIC well #12363 – Astrid-Ongstad 14-22 in Williams County, ND.

After a close match was obtained, the thermal conductivity values of each formation were adjusted until the modeled temperatures fell close to the measured profile. These thermal conductivity values were then used in the other three methods and corresponding algorithms to calculate heat flow as described below. It should be noted that the heat flow of the upper 1 to 1.5 km was adjusted by a factor of about 90% to account for cooler surface temperatures during recent glacial periods and subsequent post-glacial warming per Majorowicz et al. (2012) and Gosnold et al. (2011).

The second method used equation (1) and heat flow for each formation was calculated using the thermal conductivities from the graphical method discussed above, and initial formation thickness obtained from the North Dakota Industrial Commission's (NDIC) Scout Ticket database (https://www.dmr.nd.gov/oilgas/ subscriptionservice.asp). Formation thicknesses were subsequently adjusted by evaluating the gamma-ray profile from each well to select formation tops. An average heat flow for all of the formations was then calculated. A weighted average was also determined by calculating a weighted thermal conductivity on the basis of formation thickness divided by the total well depth:

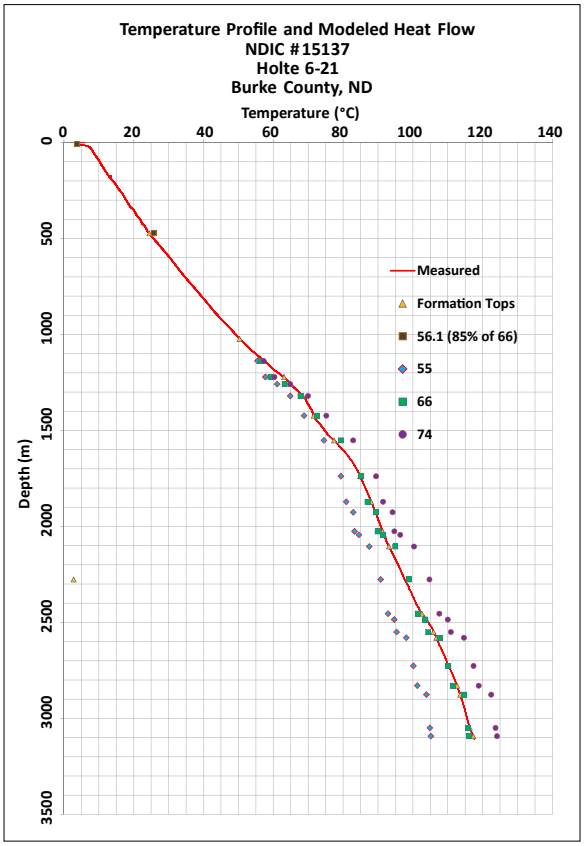

Figure 6. Measured temperature profile and modeled estimates using various assumed heat flow values. After a close was match is obtained, values of thermal conductivity are adjusted to further refine/match the measured profile. Heat flow units are mW m^{-2}.

$$Q = \lambda_w (\Delta T_t/\Delta Z_t); \text{ and} \quad (4)$$

$$\lambda_w = \lambda_1 * \Delta Z_1/\Delta Z_t + \lambda_2 * \Delta Z_2/\Delta Z_t + \ldots \lambda_n * \Delta Z_n/\Delta Z_t, \quad (5)$$

where:

λ_w = weighted thermal conductivity;

ΔT_t = temperature change from surface to bottom of well;

ΔZ_t = total depth of well; and

n, Z_n, and λ_n are as before.

An example of the results is presented in Table 1. In addition, for comparison purposes, average heat flow and weighted heat flow estimates were calculated using the thermal conductivity values utilized by Nordeng and Nesheim (2011) and Nordeng (2014), the results of which are also presented in Table 1. Nordeng arrived at his thermal conductivity values by utilizing a digitized version of the North American heat flow map published by Blackwell and Richards (2004) and back calculating the thermal conductivity values for each formation from the Rauch Shapiro Fee #21-9 well (NDIC #7591) located in Billings County, North Dakota.

The third approach employed the methodology of Bullard (1939), as cited by Beardsmore and Cull (2001). This method uses what Bullard refers to as the Thermal Resistance (R) plotted against the temperature. The thermal resistance is defined as:

$$R_i = R_{(i-1)} + \Delta Z_i/\lambda_i, \quad (6)$$

Table 1. Example calculations from NDIC 15137 – Holte 6-21, Burke County, ND.

Formation	Depth (Z)	ΔZ	Temp (T)	ΔT	λ^1	$\lambda_N{}^2$	$\lambda_{wtd}{}^3$	$\lambda_{Nwtd}{}^4$	$\Delta Z_i/\lambda$	R_i	$\lambda_{hi}{}^5$	$grad_i$	$Q_{graph}{}^6$	$Q_2{}^7$	$Q_N{}^8$	$Q_{Bullard}{}^9$	$Q_{hi}{}^{10}$
	(m)		(°C)		W m^{-1}K^{-1}				W K^{-1}		W m^{-1}K^{-1}	°C km^{-1}	mW m^{-2}				
FU/HC/FH[11]	6.7	465.7	3.7	19.9	1.20	1.72	0.18	0.26	388.11	388.11				51.1	73.3		
Pierre	472.4	465.4	23.5	22.5	1.50	1.62	0.22	0.24	310.29	698.40	0.68	42.62		72.5	78.4		28.8
Niobrara	937.9	199.6	46.0	8.9	0.80	1.62	0.05	0.10	249.56	947.95	0.99	45.49		35.6	72.0		45.0
Greenhorn	1137.5	84.1	54.9	8.2	1.20	1.62	0.03	0.04	70.10	1018.06	1.12	45.31		117.0	157.9		50.6
Mowry	1221.6	37.2	63.1	1.9	0.90	1.80	0.01	0.02	41.32	1059.37	1.15	48.92		46.5	93.0		56.4
Newcastle	1258.8	61.3	65.0	3.5	1.10	1.80	0.02	0.04	55.70	1115.07	1.13	49.01		62.6	102.5		55.3
Inyan Kara	1320.1	103.0	68.5	3.1	1.60	2.35	0.05	0.08	64.39	1179.46	1.12	49.38		48.1	70.7		55.3
Swift	1423.1	128.3	71.6	5.8	2.40	2.10	0.10	0.09	53.47	1232.93	1.15	47.97		108.7	95.1		55.4
Rierdon	1551.4	187.1	77.4	7.0	2.50	2.10	0.15	0.13	74.86	1307.78	1.19	47.75		94.0	78.9		56.6
Spearfish	1738.6	132.6	84.5	3.6	1.50	3.04	0.06	0.13	88.39	1396.18	1.25	46.65		40.7	82.4		58.1
Kibbey	1871.2	54.9	88.1	1.3	1.80	3.64	0.03	0.06	30.48	1426.66	1.31	45.26		41.4	83.7		59.4
Madison	1926.0	99.4	89.3	2.0	3.05	3.45	0.10	0.11	32.58	1459.24	1.32	44.63		62.2	70.4		58.9
Ratcliffe	2025.4	18.0	91.3	0.4	2.40	3.45	0.01	0.02	7.49	1466.73	1.38	43.43		51.9	74.6		60.0
Last Salt	2043.4	61.6	91.7	1.4	3.30	3.45	0.07	0.07	18.66	1485.39	1.38	43.24		76.2	79.7		59.5
Frobisher	2104.9	171.3	93.2	4.5	3.60	3.45	0.20	0.19	47.58	1532.97	1.37	42.65		94.6	90.6		58.6
Lodgepole	2276.2	178.3	97.7	5.0	3.50	3.45	0.20	0.20	50.95	1583.91	1.44	41.41		97.2	95.8		59.5
Bakken	2454.6	30.8	102.6	1.3	1.00	4.00	0.01	0.04	30.78	1614.70	1.52	40.42		41.9	167.5		61.4
Three Forks	2485.3	64.6	103.9	2.0	2.40	4.00	0.05	0.08	26.92	1641.62	1.51	40.44		75.5	125.9		61.2
Birdbear	2550.0	29.9	105.9	0.8	1.50	4.00	0.01	0.04	19.91	1661.54	1.53	40.21		42.1	112.3		61.7
Duperow	2579.8	146.6	106.8	3.5	3.40	4.00	0.16	0.19	43.12	1704.66	1.51	40.07		81.4	95.8		60.6
Souris River	2726.4	103.3	110.3	2.4	2.90	3.09	0.10	0.10	35.63	1740.29	1.57	39.20		67.5	71.9		61.4
Dawson Bay	2829.8	46.6	112.7	0.9	2.20	3.09	0.03	0.05	21.20	1761.48	1.61	38.62		42.2	59.3		62.0
Prairie Evaporite	2876.4	173.1	113.6	2.7	4.20	2.18	0.23	0.12	41.22	1802.70	1.60	38.30		66.4	34.5		61.1
Winnepegosis	3049.5	43.0	116.3	1.0	2.70	2.83	0.04	0.04	15.92	1818.62	1.68	37.02		61.4	64.4		62.1
Interlake	3092.5	15.2	117.3	0.3	3.00	3.72	0.01	0.02	5.06	1823.68	1.70	36.82		67.0	83.1		62.4
Bottom of Well	3107.7		117.6														
						Σ =	2.15	2.45									
Notes											Average			65.834	88.548		57.145
1 - Thermal conductivity derived from graphical method											Wtd Average6			78.846	90.224		
2 - Thermal conductivity used by Nordeng and Nesheim (2011) and Nordeng (2014)											Shallow		66.7			46.9	41.49
3 - Weighted average of graphical thermal conductivity											Deep		74.1			66.2	59.381
4 - Weighted average of Nordeng's thermal conductivity																	
5 - Harmonic mean of thermal conductivity																	
6 - Heat flow derived from graphical method																	
7 - Heat flow derived from Equation 1 for each formation																	
8 - Heat Flow derived from Equation 1 and Nordengs λ																	
9 - Heat flow derived from Bullard's Method																	
10 - Heat flow derived using harmonic mean method																	
11- FU/HC/FH - Fort Union Group/Hell Creek Formation/Fox Hills Formation combined																	

where:

R_i = thermal resistance of formation i;

ΔZ_i = depth range (formation thickness); and

λ_i = formation thermal conductivity.

Heat flow is determined by calculating the slope of the best fit line of temperature versus thermal resistance as illustrated in Figure 7. As in method 1, separate slopes were calculated for the shallow portions (upper 1 to 1.5 km) of the well bore that have been influenced by Pleistocene glacial climates and deeper portions that may be more representative of heat flow within the basin that has not been influenced by climatic changes. Results of example calculations are presented in Table 1.

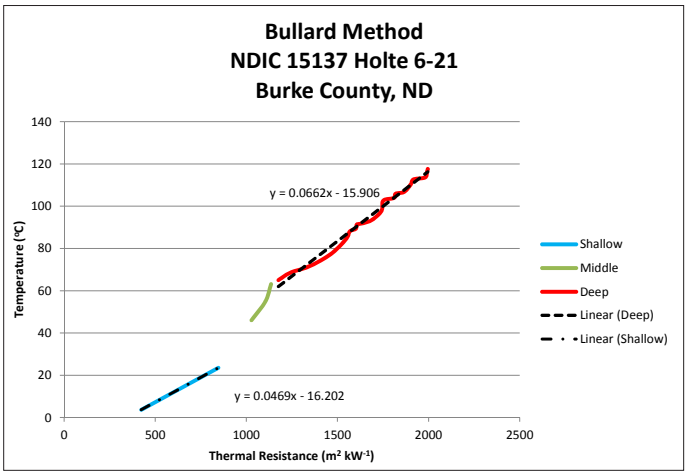

Figure 7. Example of a Bullard Plot. Slope of best fit line is the heat flow.

The last method employed to estimate heat flow was to determine the harmonic mean of the thermal conductivity as described by Beardsmore and Cull (2011). This method calculates the harmonic mean of the thermal conductivity by dividing the depth to the top of each formation by the thermal resistance calculated using equation (6):

$$\lambda_{hi} = Z_i/R_i \tag{7}$$

where:

λ_{hi} = harmonic mean thermal conductivity;
Z_i = depth to top of formation; and
R_i = as above.

Next, the gradient is determined by dividing the difference between the temperature at the top of the formation and the temperature at the top of the stratigraphic column by the difference between the depth to the top of the formation and the depth to the top of the stratigraphic column under consideration:

$$grad_i = (T_i - T_s)/ (Z_i - Z_s), \tag{8}$$

where:

$grad_i$ = temperature gradient to top of formation i;
T_i = temperature at top of formation i;
T_s = temperature at top of stratigraphic column;
Z_i = depth to top of formation i; and
Z_s = depth to top of stratigraphic column.

Heat flow for each formation is then calculated by taking the product of harmonic thermal conductivity times the gradient:

$$q_{hi} = \lambda_{hi} * grad_i. \tag{9}$$

An example calculation is provided in Table 1. Average values for each well are given in Table 2 and again, values for shallow (< 1.5 km) and deep segments were calculated separately. Figure 8 presents a map showing the average of the values obtained from the graphical, harmonic mean, Bullard and the weighted average methods.

Discussion and Conclusions

Results of the preliminary study are presented in Table 2. While there is general agreement in calculated heat flow values between the various methods presented above, the results are largely predicated upon initial assumptions of either heat flow, thermal conductivity, or both. This is clearly illustrated by the large discrepancies between the values obtained by using Nordeng's thermal conductivity values and the values obtained using the other methods. In addition, the average and weighted average of method 2 results in relatively large differences in heat flow between formations. With the exception of the surface temperature forcing signal resulting from global climatic variations during the last ice age and subsequent post-glacial warming, calculated heat flow across the various formations should be nearly equivalent, if the thermal conductivity values used in the analyses are close to actual values.

The results of the harmonic method described above seem to yield the most consistent heat flow values between the formations (Table 1). However this issue still reduces down to a "chicken or egg" scenario in that heat flow and thermal

conductivity are dependent upon each other and inaccurate assumptions of one profoundly affects the other. While we are confident in the measurements obtained during this study with respect to thermal gradients, it is evident that additional information with regard to thermal conductivities of the geologic formations will be required to accurately determine heat flow within the Williston Basin. Geologic formations can often be differentiated on the basis of "marker" beds; however there can be wide variations in mineralogy, lithology, porosity, permeability, density, etc., depending upon depositional environment, depth of burial, secondary processes, etc., from one location to another within the same formation.

These criteria can profoundly influence thermal conductivity and therefore greatly influence the calculated heat flow.

Table 2. Summary of Heat Flow Estimates by Well.

Well #	Well Name		Tabular	Nordeng's	Bullard	Harmonic	Graphical	Average
			mW m^{-2}					
2139	**NSCU V-706** Northeast of Newburg, ND	Average	43.5	66.5		26.7		
		Wtd Avg.	46.9	74.6				
		Shallow[a]			20.4	26.7	48.0	35.5
		110%[b]	51.59		22.44	29.37	52.8	39.1
8005	**Sivertson 29-23R1** Southeast of Keene, ND	Average	60.2	80.9		54.4		
		Wtd Avg.	73.2	94.4				
		Shallow			35.3	39.6	51.0	
		Deep[c]			58.4	55.7	60.0	61.8
16376	**Vernie Chapin 32-21** Southeast of Keene, ND	Average	59.8	87.6		61.7		
		Wtd Avg.	72.7	93.0				
		Shallow			45.9	45.6	51.0	
		Deep			58.8	63.0	60.0	63.6
9653	**Cutlip #1** Northwest of Alexander, ND	Average	50.6	75.4		50.4		
		Wtd Avg.	54.5	74.8				
		Shallow			38.0	37.1	45.0	
		Deep			51.9	52.3	50.0	52.2
10103	**Iverson State A-1** Northwest of Alexander, ND	Average	49.9	76.3		57.7		
		Wtd Avg.	54.9	74.9				
		Shallow			89.4	45.1	45.5	
		Deep			51.5	59.5	50.5	54.1
12363	**Astrid-Ongstad** Northeast of Tioga, ND	Average	52.0	82.2		50.1		
		Wtd Avg.	61.0	87.2				
		Shallow			46.9	37.0	51.6	
		Deep			55.9	51.3	54.0	55.6
16182	**2004 JV-P NDCA 7** North of Tioga, ND	Average	53.8	86.5		45.8		
		Wtd Avg.	56.6	85.2				
		Shallow			37.1	33.1	44.1	
		Deep			52.7	47.8	49.0	51.5
13666	**Rieder 1-9 SWD** North of Williston, ND	Average	52.0	79.4		43.2		
		Wtd Avg.	51.4	77.9				
		Shallow			53.0	32.6	45.3	
		Deep			50.3	45.0	50.3	49.3
15137	**Holte 6-21** Southwest of Columbus, ND	Average	59.5	88.5		57.1		
		Wtd Avg.	71.8	90.2				
		Shallow			46.9	56.6	56.1	
		Deep			66.2	59.9	66.0	66.0
15593	**FHMU K-810** West of Fryburg, ND	Average	56.1	88.3		52.4		
		Wtd Avg.	60.6	87.9				
		Shallow			56.4	40.0	45.0	
		Deep			55.3	54.5	50.0	55.1
17043	**St. Andes 151-89-2413H-1** Southeast of Parshall, ND	Average	49.1	60.8		42.0		
		Wtd Avg.	59.1	69.5				
		Shallow			48.6	28.7	54.3	
		Deep			57.2	42.6	60.3	54.8

Notes:
a - Shallow is the upper 1 to 1.5 km that may reflect influence of Paleoclimate and subsequent post-glacial warming.
b - Glacial periods may reduce heat flow by 10 to 15% per Majorowicz et al. (2012) and Gosnold et al. (2011).
c - Deep are values calculated below 1 to 1.5 km

Future Work

The NDGS currently has plans to log an additional 20 to 30 wells over the next one to two years. However, as noted above, some funding may be redirected to obtain additional thermal conductivity information from the wells that are being logged. Ideally, thermal conductivity values from core samples obtained from the wells that are logged would allow for the calculation of a reasonable estimate of heat flow from specific locations. This may also allow for better estimates of thermal conductivity by reverse modeling for the various formations at these locations that do not have core samples. This information, combined with thermal maturity estimates obtained by other methods (Nordeng and Nesheim, 2011) would provide better estimates of heat flow within the Williston Basin, better predictions of thermal maturity and the geothermal potential of the region.

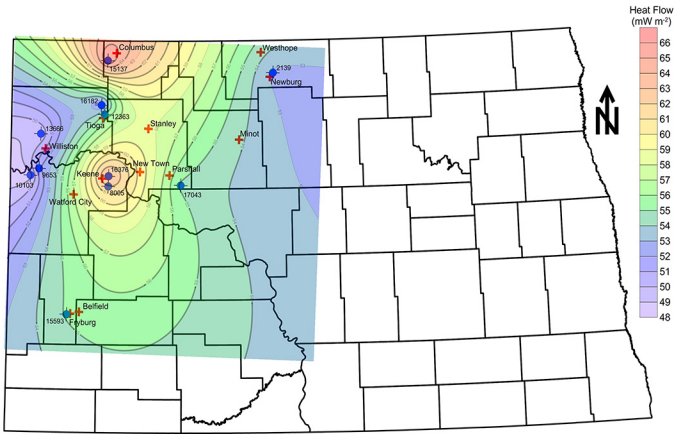

Figure 8. Mean heat flow of the graphical, harmonic mean, the Bullard method and the weighted average methods.

Acknowledgements

Funding for this project was provided by the North Dakota Petroleum Council and the State of North Dakota. We would also like to acknowledge Hess Corporation, Jordan Exploration, Inc., Missouri Basin Well Service Inc., Enduro Operating, LLC, Liberty Resources LLC, and Encore Energy Partners Operating LLC for their cooperation and assistance in allowing us access to their wells.

References

Blackwell, D.D., and M.C Richards, 2004, Geothermal map of North America 2004: American Association of Petroleum Geologists, Tulsa, OK.

Beardsmore, G.R., and J.P. Cull, 2001, Crustal heat flow, a guide to measurement and modelling: Cambridge University Press, Cambridge, United Kingdom, 324 pp.

Bullard, E.C., (1939), Heat flow in South Africa: Proceedings of the Royal Society of London, A, 173, p. 428-450.

Cooper, L.R., and C. Jones, 1959, The determination of virgin strata temperatures from observations in deep survey boreholes: Geophysical Journal of the Royal Astronomical Society, v. 2, p. 116-131.

Lachenbruch A.H., and M.C. Brewer, 1959, Dissipation of the temperature effect of drilling a well in Artic Alaska, U.S. Geological Survey Bulletin, 1083-C, p. 73-109.

Gosnold, W.D., M.R. McDonald, R. Klenner and D. Merriam, 2012, Thermostratigraphy of the Williston Basin, GRC Transactions, v. 36, p. 663-670.

Gosnold, W., J. Majorowicz, R. Klenner and S. Hauck, 2011 Implications of post-glacial warming for northern hemisphere heat flow, Geothermal Resources Council Transactions, v. 35, p. 795-799.

Gosnold, W., and A. Crowell, 2014, Heat flow and geothermal research in the mid-continent, 2014, Geothermal Resources Council Transactions, v. 38, p. 127-131.

Majorowicz, J., W. Gosnold, A. Gray, J. Safanda, R. Klenner, and M. Unsworth, 2012, Implications of post-glacial warming for Northern Alberta heat flow – correcting for the underestimate of the geothermal potential, Geothermal Resources Council Transactions, v. 36, p. 693-698.

McDonald, M.R., and S.H. Nordeng, 2014, Temperature logging in the Williston Basin; North Dakota Department of Mineral Resources Geo News, v.41, n. 2, p. 11-13.

Nordeng, S.H., and T.O. Nesheim, 2011, Determination of subsurface temperatures and the fraction of kerogen converted to petroleum within the Rauch Shapiro Fee #21-9, Billings Co., ND, North Dakota Geological Survey, Geological Investigation 146.

Nordeng, S.H., 2012, Determination of activation energy and frequency factor for samples of the Bakken Formation (Mississippian-Devonian) Williston Basin ND: North Dakota Geological Survey, Geological Investigation 163, 15 pp.

Nordeng, S.H., 2013, Evaluating source rock maturity using multi-sample kinetic parameters from the Bakken Formation (Mississippian-Devonian) Williston Basin ND, North Dakota Geological Survey, Geological Investigation 164, 19 pp.

Nordeng, S.H., 2014, Building the science for advancing oil and gas exploration and development in the Williston Basin, North Dakota Department of Mineral Resources Geo News, v.41, n. 1, p. 14-18.

Nuccio, V.F., and C.E. Barker, eds., 1990, Applications of thermal maturity studies to energy exploration, Society of Economic Paleontologists and Mineralogists, Rocky Mountain Section, 174 pp.

Prensky, S., 1992, Temperature measurements in boreholes: an overview of engineering and scientific applications, The Log Analyst, v. 33, no. 3, p. 313-333.